Within Subject Reproducibility and Between Subject Variability of Super-Resolution Track-Weighted Imaging

Lisa Willats[1], David Raffelt[1], Robert Elton Smith[1,2], Jacques-Donald Tournier[1,2], Alan Connelly[1,2], and Fernando Calamante[1,2]

[1]*Brain Research Institute, Florey Neuroscience Institutes, Melbourne, Victoria, Australia,* [2]*Department of Medicine, University of Melbourne, Victoria, Australia*

Background: Recently several novel image contrasts derived from whole-brain fibre-tracking data (tractograms) have been introduced [1-3]. The novel contrasts of these track-weighted imaging (TWI) methods may provide important information for clinical studies [3, 4]. However, before they can be used reliably to generate quantitative measures, it is important to characterise the *within*-subject (WS) *intra*-session and *inter*-session reproducibility, and *between*-subject (BS) variability. To date, BS variability has only been studied for a couple of specific contrasts [3], and only *inter*-session WS reproducibility on a single subject [3]. In this work we investigate the WS reproducibility (both *intra*-session and *inter*-session), and BS variability of TWI for a number of different contrasts across multiple subjects.

Methods: Data Acquisition: 3 diffusion MRI datasets (60 diffusion directions, b=3000s/mm^2, 2.5mm isotropic voxels) were acquired for each of 8 healthy adults on a 3T Siemens Trio. For each subject, 2 datasets were acquired in succession in a single session (scans 1 and 2); a third (scan 3) was acquired on a different day.

Data Processing: Pre-processing steps included: upsampling by a factor of two [5]; EPI distortion correction [6]; motion correction [5]; bias-field correction [5]; and intensity normalisation [5]. The proceeding analysis was carried out using in-house software based on MRtrix (http://www.brain.org.au/software). Constrained Spherical Deconvolution (CSD) [7] was used to estimate the Fibre Orientation Distribution (FOD) in each voxel, using the group average response function [5]. Tractograms of 5-million tracks were generated using probabilistic streamlines [8].

Track-weighted imaging: For each dataset, Track-weighted (TW) images with contrast generated from the fractional anisotropy (FA) map, the mean apparent diffusion coefficient (ADC) map, the apparent fibre density (AFD) [5] map, and a unity map (uniform image value of 1) (corresponding to track-density imaging (TDI) [1,2]), were created. The TW images were formed by considering the value of the associated map (e.g. FA) along each streamline of the tractogram [2]: for each super-resolution grid element [1] the neighbourhood Gaussian weighted mean of the map value (e.g. FA) along each streamline passing through the voxel was calculated; the TW image voxel intensity is the mean of these values for all streamlines passing through that voxel. *Three Gaussian neighbourhood weightings* were considered with FHWMs of 15mm, 40mm and 100mm, denoted by TW(FWHM), chosen to generate a sub-range of contrasts [2]. The TW images were computed at *two isotropic resolutions* of 1.25mm (native upsampled resolution) and 0.625mm (super-resolution), denoted by TW$^{\text{resolution}}$. Symmetric diffeomorphic FOD registration [9] was used to create a population-specific template using all 24 datasets. TW-FA and TW-ADC were computed in native space then normalised to the template. TW-AFD and TDI were computed from registered tractograms, with relevant AFD maps created from registered and modulated FOD images [5].

Statistical Analysis: For each TW image, the total WS variance (σ^2_{WS}) of each voxel value y across the N=8 subjects was calculated *intra*-session (WS_{12}): $\sigma^2_{WS12}=(1/N)\sum^{N}_{n=1}0.5(y_{n1}-y_{n2})^2$ (scan 1 vs. scan 2) and *inter*-session (WS_{13}): $\sigma^2_{WS13}=(1/N)\sum^{N}_{n=1}0.5(y_{n1}-y_{n3})^2$ (scan 1 vs. scan 3). Similarly, the total BS variance (σ^2_{BS}) for each voxel was calculated: $\sigma^2_{BS}=(1/N-1)\sum^{N}_{n=1}2(\bar{y_n}-\mu)^2$, where $\bar{y_n}=0.5(y_{n1}+y_{n2})$ and $\mu=\sum^{N}_{n=1}\bar{y_n}/N$. From these variances, voxel-wise maps of the coefficient of variation, $CV=(\sigma/\mu)\times100\%$, reproducibility index, $RI=\sqrt{2}\times1.96\sigma$, and intraclass correlation coefficient, $ICC=(\sigma^2_{BS}-\sigma^2_{WS})/(\sigma^2_{BS}+\sigma^2_{WS})$, were computed.

Results: Table 1 gives the median *CV* and *ICC* for all TW image contrasts analysed. There is less variability (lower median *CV*) and better consistency (higher median *ICC*) for TW$^{1.25mm}$ compared with TW$^{0.625mm}$, and for TW(15mm) compared with TW(40mm) or TW(100mm). There is only a small difference between *intra*-session (WS_{12}) and *inter*-session (WS_{13}) statistics. Unsurprisingly, there is less variability WS compared with BS. Figure 1 gives the percentile curves of *CV* and *ICC* for a subset of the results in Table 1 (bold cells). TW-ADC has the greatest proportion of voxels with low *CV*, whereas TW-AFD has the greatest proportion of voxels with high *ICC*. Figure 2 illustrates the regional distribution of variability for this subset of results with images of μ and *RI*. Note that due to the similarity between *intra* and *inter*-session statitites, only the *intra*-session WS_{12} images are shown. Relative to μ, *RI* is smallest for TW-ADC and largest for TDI. Note that the μ and *RI* images of each TW contrast have the same windowing.

	resol. (mm)	FWHM(mm)		15	40	100	15	40	100	15	40	100
			TDI	TW-AFD			TW-FA			TW-ADC		
CV (%)	0.625	WS_{12}	38.8	11.72	13.23	15.75	10.45	12.79	14.74	3.61	4.51	4.84
		WS_{13}	39.7	12.47	13.90	16.36	10.96	13.26	15.20	3.90	4.74	5.07
		BS	92.6	41.62	41.71	42.56	30.63	29.59	30.41	13.01	11.69	11.26
	1.25	WS_{12}	**30.0**	**9.44**	10.37	12.22	**8.94**	10.59	12.15	**3.00**	3.70	3.95
		WS_{13}	**31.1**	**10.31**	11.28	13.05	**9.39**	11.01	12.57	**3.26**	3.90	4.14
		BS	**342.8**	**38.08**	38.37	38.88	**27.02**	26.06	26.67	**12.02**	10.73	10.29
ICC	0.625	WS_{12}	0.54	0.82	0.80	0.76	0.72	0.63	0.57	0.79	0.67	0.62
		WS_{13}	0.53	0.80	0.78	0.75	0.70	0.61	0.56	0.76	0.65	0.60
	1.25	WS_{12}	**0.62**	**0.86**	0.85	0.82	**0.76**	0.67	0.62	**0.84**	0.74	0.69
		WS_{13}	**0.60**	**0.85**	0.83	0.80	**0.74**	0.66	0.60	**0.81**	0.71	0.67

Table 1: Median *CV* and *ICC*.

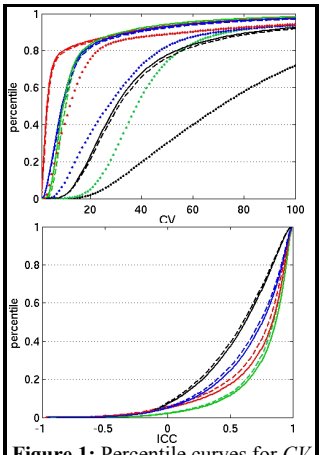

Figure 1: Percentile curves for *CV* (top) and *ICC* (bottom). Black =TDI; green=AFD; blue=FA; red=ADC. solid=*intra*-session WS_{12}; dashed=*inter*-session WS_{13}; dotted= BS

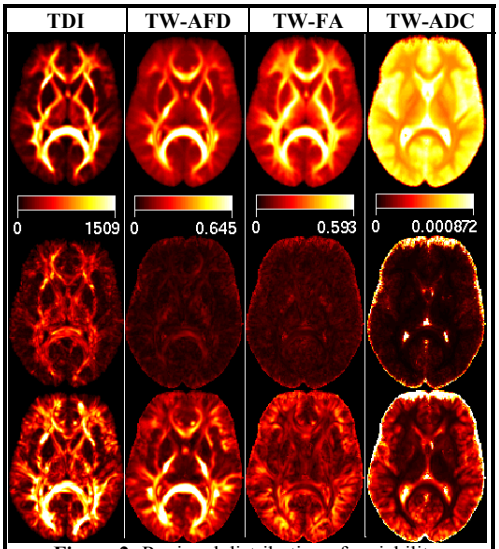

Figure 2: Regional distribution of variability. Top to bottom: μ; *RI*(WS_{12}); *RI*(BS).

Discussion: As expected, and in concordance with ref. [3], TDI (which depends on the number of tracks in a given voxel) had poor WS and BS reproducibility. TDI is therefore not ideal for quantitative analysis and should primarily be used for its rich anatomical detail [1]. The lower WS reproducibility of TW-FA compared with TW-ADC is not surprising given that without track-weighting, FA has been found to have lower reproducibility than ADC [10]. While we used a sophisticated registration technique [9], the difference between the WS and BS variation may still be exacerbated by imperfect registration in the cortical areas. Even so, BS variation is still greater than WS within the well aligned major fibre bundles (Figure 2). Although TW-ADC has the lowest *CV*, the *ICC* of the TW-AFD is greatest due to the proportionally larger BS *CV* (c/w WS *CV*) (Table 1). The high BS variability of TW-AFD in the major fibre bundles (e.g. the corpus callosum, Figure 2) indicates natural variation *between*-subjects, since here we expect registration errors to be small. This variation is due to FOD modulation in the AFD registration step, which causes the AFD maps to encapsulate variation in the spatial extent of fibre bundle widths, as well as their diffusion properties. For all TW contrasts, the similarity between the *intra*-session and *inter*-session reproducibility indicates that TWI is robust to subject repositioning.

Conclusion: We have presented an investigation into the *within*-subject reproducibility and *between*-subject variation of several TW image contrasts. This provides important information concerning their utility and sensitivity for longitudinal studies and group comparison.

References: [1] Calamante et al. Neuroimage 2010:53:1233. [2] Calamante et al. doi:10.1016/j.neuroimage.2011.08.099. [3] Pannek et al. Neuroimage 2011:55 :133. [4] Bozzali et al. Neuroimage 2011:54:2045. [5] Raffelt et al. doi:10.1016/j.neuroimage.2011.10.045. [6] Holland et al. Neuroimage 2010:50:175. [7] Tournier et al. Neuroimage 2007:35:1457. [8] Tournier et al. ISMRM 2010:1670. [9] Raffelt et al. Neuroimage 2011:56:1171. [10] Farrell et al. JMRI 2007:26:756.